LA-UR-03-1528
*Approved for public release;
distribution is unlimited.*

Title:

A CONSISTENT MATERIAL PARAMETER SET FOR DYNAMIC LOADING OF TANTALUM

Author(s):

T.A. Mason, P.J. Maudlin and B.L. Henrie

Submitted to:

A CONSISTENT MATERIAL PARAMETER SET FOR DYNAMIC LOADING OF TANTALUM

T.A. Mason[1], P.J. Maudlin[1] and B.L. Henrie[1]
Technical Staff Member[1]
Los Alamos National Laboratory, PO Box 1663, MS G755, Los Alamos, New Mexico, 87545

I. Abstract

The high-rate failure response of a material has most often been studied through the use of shock loaded discs in near one-dimensional tests. Shock loading has applied the rapid loading rates and shock amplitudes that approximate ordnance applications, but not usually with accurate wave profiles or dimensionality. In particular, plate-on-plate experiments have been employed to study the effect of pulse duration and amplitude on the progression of damage from void nucleation to coalescence to macroscopic cracking and total failure. This scheme is idealized as employing a square-top pulse in an almost one-dimensional experiment where the interior of the sample can experience a hydrostatic tensile stress and the strain is assumed to be uniaxial. These tests can be well constrained and are very repeatable. These tests also have a respectable history in the shock physics community and the interpretation of the free surface velocities of the impacted discs have long been used to infer details of the progression of damage in the target's interior. Additionally, post-mortem examination of incipiently failed discs has been performed to obtain data for developing and validating void nucleation and coalescence models for use in larger scale modeling efforts. Recent experiments at Los Alamos National Laboratory cast some doubt on the appropriateness of relying too strongly on the results of plate-on-plate shock experiments to develop or validate damage models for use in modeling general ordnance applications where significant amounts of shear can occur. This can yield damage and failure mechanisms that are significantly different than those present in plate-on-plate tests.

II. Three dimensional shock experiments

In recent months, a series of explosively loaded disc experiments have been performed at Los Alamos in an effort to demonstrate the use of proton radiography in visualizing internal damage and failure at multiple instances during a single dynamic experiment. The test series included tin, copper, aluminum and tantalum discs. We are particularly interested in the tantalum tests as they used plate material that has had its elastic and plastic properties, yield surface shape and equation of state all previously determined.

The schematic details of the experiments are shown in Figure 1. A two inch (50.8 mm) diameter metal disc is glued to an identical diameter disc of PBX 9501 explosive. In the case of the tantalum experiments, the metal discs were 0.175 inches (4.45 mm) thick and the explosive was one half inch (12.7 mm) thick. A detonator was attached to the center of the bottom face of the high explosive charge and the assembly was held in a Lexan plate by friction. Note that neither the explosive charge nor the explosive gas products were confined by a case or enclosure. This results in no secondary shock of the disc from reflected shocks in the detonation products. Each disc was accelerated upwards by the explosive charge and the free surface velocity was measured using VISAR techniques. Note that the Chapman-Jouguet pressure for PBX 9501 is approximately 35 GPa but the shock match pressure for a normal shock passing from the high-explosive to a tantalum solid is about 61 GPa [1]. Shock obliquity angles up to about 45° reduce this value slightly but not to a value lower than 57 GPa.

The free surface velocity measurements of three shots are shown in Figure 2. Two shots were decelerated by impacting transparent windows made from lithium fluoride (LiF) while the third shot was allowed to fly unimpeded. The rational behind impacting the damaged discs on LiF windows was that detailed analysis of the resulting velocity changes of the tantalum/LiF interface would yield information about the 'spall' layers present in the separating disc. These velocity changes are again monitored using VISAR. A series of impacts of distinct layers would be discernible in the VISAR traces as well as the layers' thicknesses and spacing. There is good repeatability between the three shots with the recorded velocity profile being nearly identical up to the time that the first disc impacted the LiF at a stand-off of 1.58 millimeters. Neither the 1.58 mm nor the 3.68 mm stand-off experiments demonstrate the expected stair-step 'ring-down' of the sample as they impact the LiF windows.

This 'ring-down' behavior was clearly seen in tests using the other metals listed above. From this point on, the 1.58 and 3.68 millimeter stand-off experiments will be called T-18 an T-21, respectively.

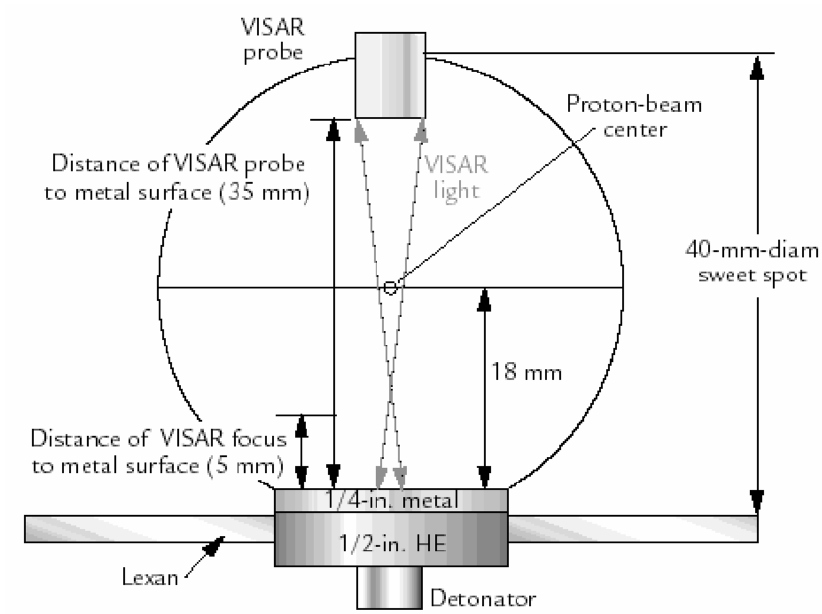

Figure 1. Schematic of explosively loaded disc experiments

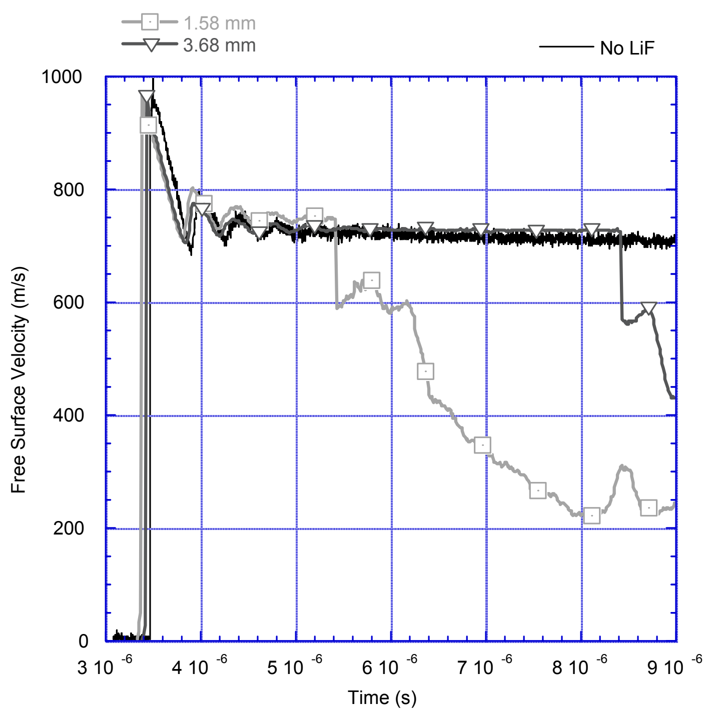

Figure 2. Free surface velocity measurements for three identically loaded tantalum disc experiments. Two discs were decelerated at standoffs of 1.58 and 3.68 mm, respectively while the third, denoted by 'No LiF' was allowed to fly unimpeded.

The classic interpretation of these free surface velocity traces is that the discs have 'spalled' or opened up a free surface in their interiors. This has trapped a portion of the energy from the shock wave in the 'spall' layer which now 'rings' or vibrates with a much smaller period than the initial sample. Historically, the velocity trace has been used as definitive evidence that a spall had occurred. This assumption has been particularly convenient when the damaged sample has not been recoverable.

III. Tensile Plasticity

A rate-dependent formulation of the Tensile Plasticity (TEPLA) damage model [2,3] has been implemented in a dynamic finite element code. This implementation uses a Gurson-type flow surface that is 'softened' by accumulated damage. This flow surface uses temperature and strain-rate dependent constitutive models and anisotropic yield surface information to more accurately capture the response of anisotropic, rate-dependent materials. Voids are allowed to grow in proportion to the volumetric deformation gradient and the accumulation of both void fraction and accumulated strain impact the determination of whether an individual element has failed during a simulation cycle.

As noted above, the selection of this particular tantalum plate as stock for these shots was very fortunate as it has been carefully studied in the past and most of the material parameter sets needed to model these tests have been previously determined. This data included the elastic constants, yield surface shape and the strain-rate and temperature dependent constitutive model. Additionally, the simulations of a separate suite of tantalum plate-on-plate experiments [4] have begun in an effort to obtain a 'best-fit' TEPLA parameter set. The addition of these tests to the explosively loaded disc tests should yield a more robust TEPLA parameter set as it would address two very different boundary conditions with one parameter set.

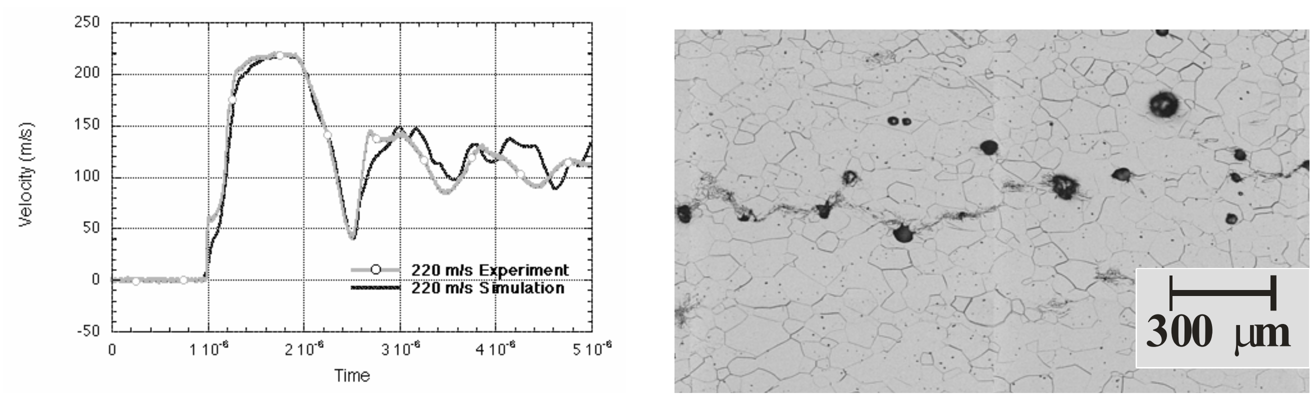

(a) (b)

Figure 3. (a) Comparison of free surface velocity traces of a plate-on-plate experiment and simulation. Both void growth and shear failure options are used in the TEPLA constitutive model. (b) Post-mortem examination of tantalum target after plate-on-plate impact at 6.3 GPa shock pressure. Maximum local porosity was estimated at 0.055.

Figure 3a shows the agreement between the initial simulation and experimental free surface velocity traces for one of the tantalum plate-on-plate experiments. These results would seem to indicate that the tantalum target plate spalled according to the classical interpretation. Figure 3b contradicts that interpretation as it shows the metallographic image of the cross section of the recovered tantalum plate. While there is a damaged region in the center of the plate, there is no clear spall plane where the sample has fractured. It seems that a layer of voids, damage and/or shear localization can act to mimic a fracture plane by reflecting some of the energy in a shock wave. It should be noted that the damage simulations predicted many failed elements in the interior of the tantalum plate but the post-mortem characterization yielded an estimate of only about 5.5% porosity. In this case, at least, TEPLA produces too much porosity and thus fails too many cells.

In modeling these disc experiments, the parameter set that was developed for use in the plate-on-plate experiments was used as a starting point for the explosively loaded disc experiments. The explosive was modeled using an appropriate date set from the material library and the effect of the detonator was duplicated by calculating the detonation break-out times and programming the corresponding burn initiation times on the appropriate nodes of the main high-explosive mesh. The artificial viscosity terms were tuned using the plate-on-plate simulation as the 'flat-top' shape of the shock wave was more constraining on the simulations than the sharp cusp of the explosive loading.

The best match between these initial, full TEPLA, runs and experiment is shown in Figure 4 denoted by 'Full Tepla'. The main features of the free surface velocity were correct but the absolute amplitude of the surface velocity where the reverberations commenced was not attainable as well as the late-time velocity was not correct. Numerous attempts were made to correctly balance the competing contributions of void growth and shear localization as programmed in TEPLA. None of these attempts yielded results that were better than that shown. One important thing to note here is that even with both void growth and strain-to-failure allowed to influence the failure of each element only a very small amount of porosity grew. The largest porosity in any element during this simulation was about 0.02 or two percent. When the two failure mechanisms are allowed to compete, void growth does not dominate the failure of elements but does drive the final solution away from being experimentally consistent.

In an attempt to more fully explore the relative potencies of the two damage mechanisms present in TEPLA, we decided to use each mechanism alone to learn how the damage in the disc would progress in each case. The first case explored was to turn off the void growth portion of TEPLA and rely solely on the strain-to-failure option defined by the Hancock-MacKenzie curve [5]. This improved result is also shown in Figure 4 denoted by 'Shear Only'. The simulated free surface velocity matches the experimental trace very well and reaches the appropriate late time velocity as well. This result is more consistent with the VISAR trace but it leads to the conclusion that the damage is most likely controlled by strain localization.

Imperfect, as this last simulation may be, it shows that a simulation using a strain-dominated failure mechanism can produce a better result than a simulation where both spall and strain can operate. The simulations using void growth alone have not been completed at this time.

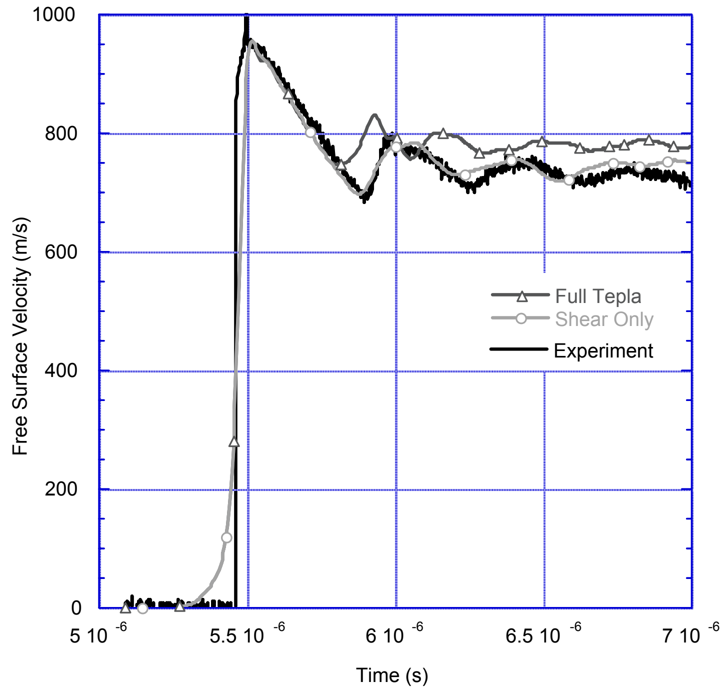

Figure 4. Comparison between experimental free surface velocity and simulation using both void growth and shear failure options, 'Full Tepla', and then only the Hancock-McKenzie shear failure option, 'Shear Only', in the TEPLA constitutive model.

IV. Post-mortem characterization of explosively loaded discs

The explosively loaded discs in the two LiF window shots were recovered from the containment tank after each shot. It is important to remember that these samples were not 'soft-caught' but were decelerated from approximately 800 meters per second to less than 100 meters per second during the impacts with the LiF windows. These samples were sectioned and mounted for examination using optical and scanning electron imaging (SEM) techniques and electron diffraction backscatter diffraction (EBSD) measurements. Figure 5 shows a reconstructed microstructure of sample T-18 using EBSD measurements on a spatially resolved grid. The false coloration is based on local lattice orientation with respect to the disc normal direction. The center of the image corresponds to the intersection of the disc center line and mid plane. There is no clear spall plane or even an array of large voids. Instead there is a network of strain localizations running across the bulk of the sample. There are a number of small voids with diameters on the order of 10 micrometers whose locations do not appear to be strongly correlated with the strain localizations. This evidence shows that while the strain dominated simulation is more consistent with the free surface measurement, it predicts too much damage, too early in the experiment.

The appearance of this microstructure is in marked contrast to that obtained from tantalum plate-on-plate experiments where the maximum shock pressure was only about 6.0 GPa. A reconstructed grain map from a different section from the sample shown in Figure 3b is shown in Figure 6. Note that the voids are very large, approximately 100 micrometers in diameter, and the location of the voids and the strain localizations are strongly correlated. This material experienced a much lower pressure but a relatively long pressure pulse, both compressive and tensile, from the 'flat-top' shock resulting from the plate impact loading.

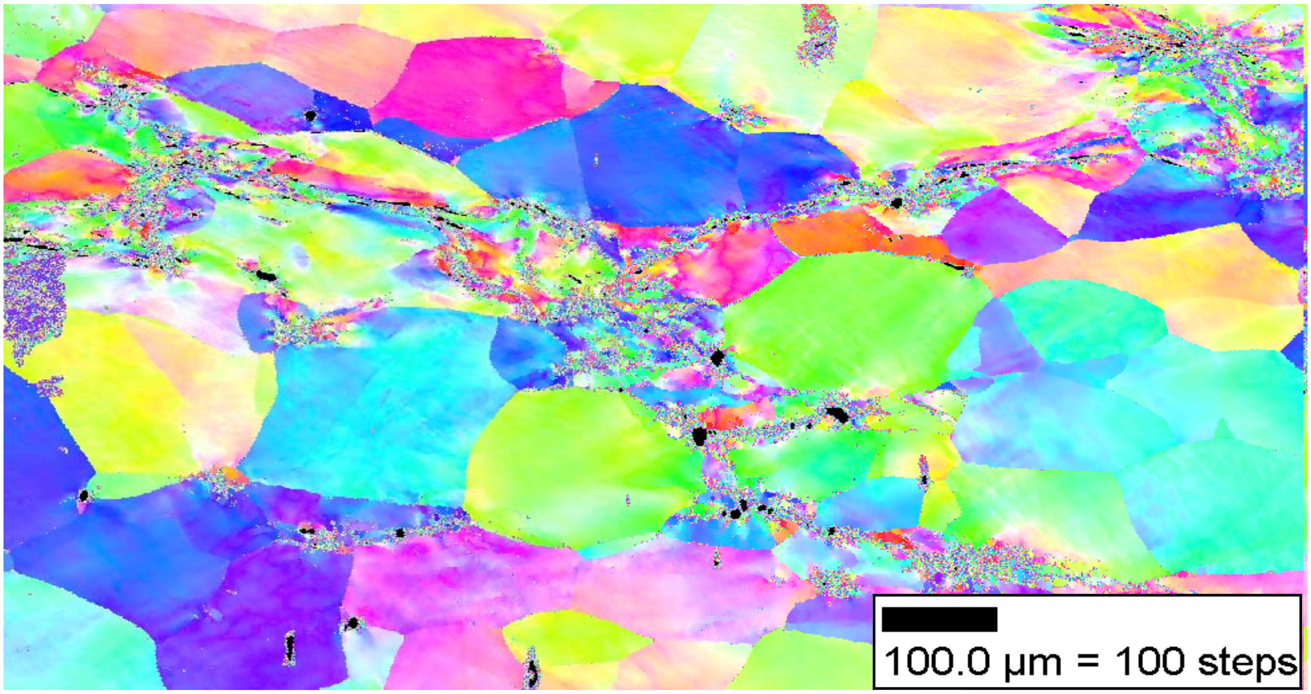

Figure 5. Reconstruction of EBSD data of sample T-18. The center of this image corresponds to the centerline and mid-plane of the disc. The voids are less than 10 μm in diameter.

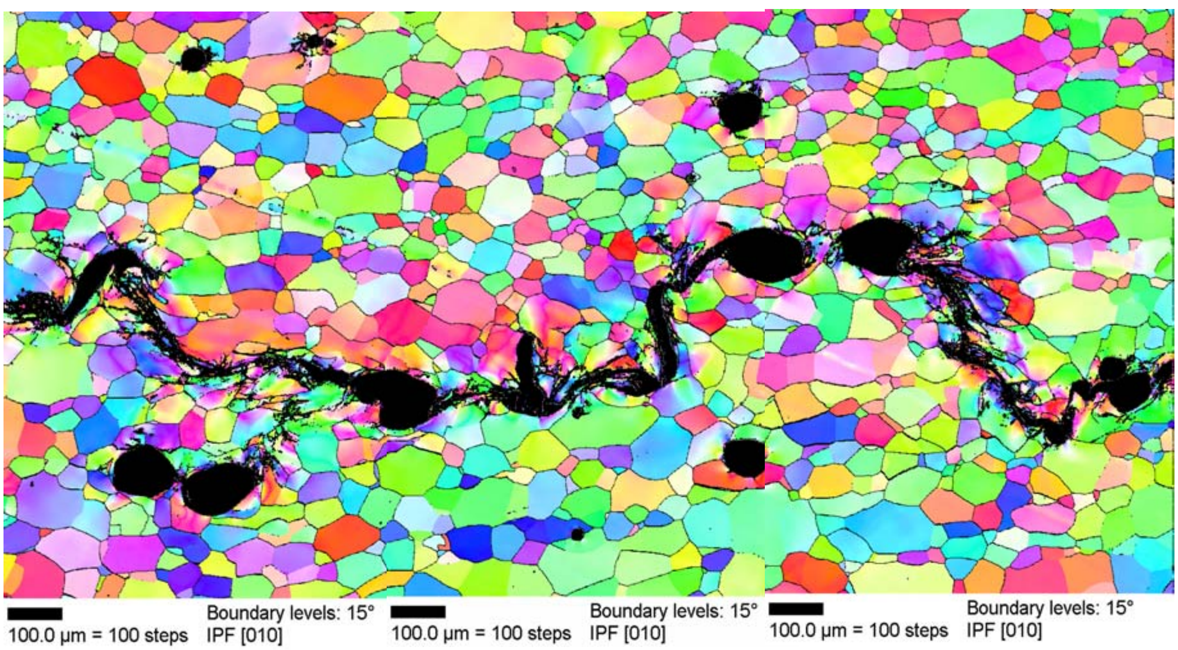

Figure 6. Reconstruction of EBSD data from the tantalum plate-on-plate sample in Figure 3b. The voids are, on average, larger than 100 μm in diameter and the strain localizations are strongly correlated with the void locations.

Away from the central damage area in sample T-21 the microstructure shows the clear transition away from the localization networks seen in sample T-18. In T-21, the bulk of the sample exhibits signs of having experienced large strain deformations not just local shear flow. Additionally, Figure 7 shows details of the macroscopic flaws or 'cracks' that have been produced by allowing the disc to fly an additional three microseconds before being decelerated. These flaws appear to be joined voids that may have nucleated on shear localizations in a manner similar to the 'void-sheeting' reported in the literature [6-11]. An important point of departure here is that this tantalum is of relatively high purity and there is no population of second phase particles or precipitates present to serve as nucleation sites for the raft or sheet of voids. Additionally, these macroscopic ‘cracks’ appear to be formed by the overlapped growth of voids and not by shear localizations and cracks running between larger voids.

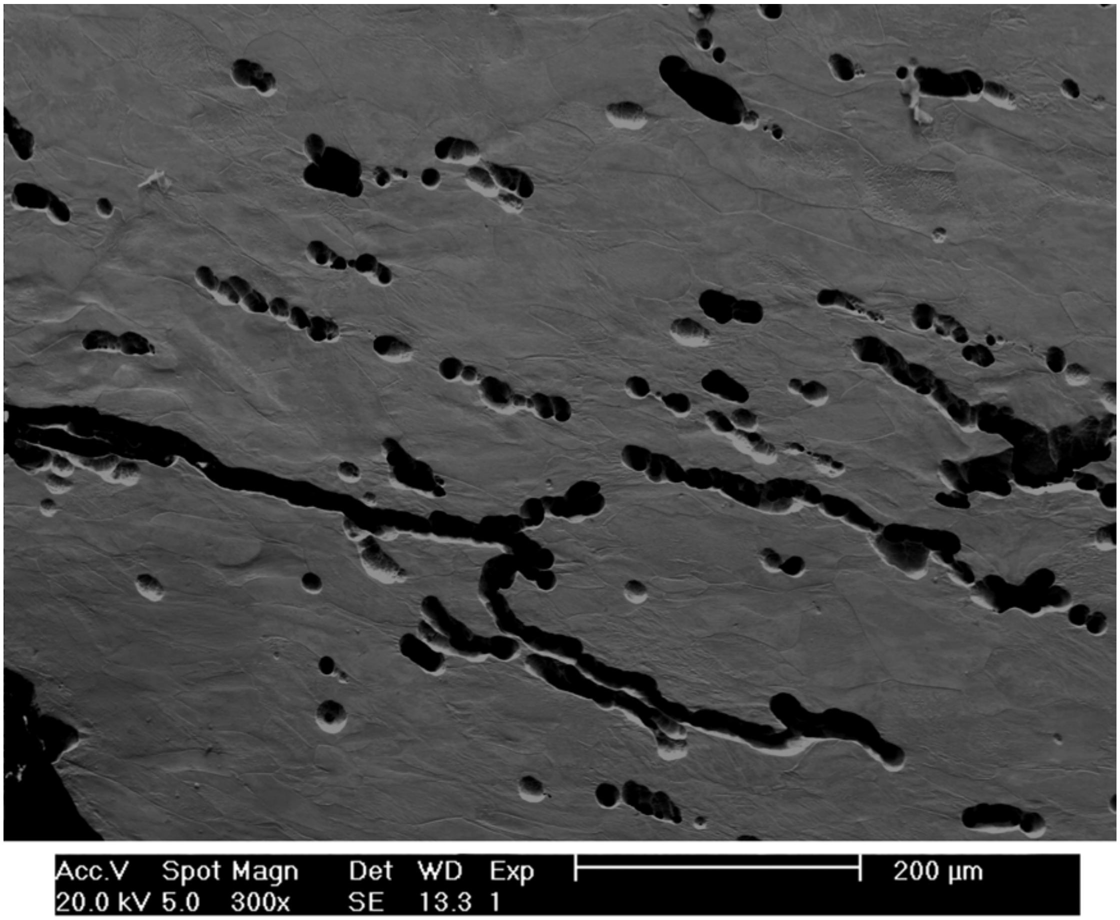

Figure 7. Back scattered electron SEM image of a typical damage zone in sample T-21. Mesoscopic ‘cracks’ appear to be locally linked void sheets.

In examining samples T-18 and T-21 an obvious question might be whether voids grew during the initial stages of the experiment but were subsequently closed or welded shut during the impacts with the LiF windows. We felt that this was unlikely due to the high melting temperature of the tantalum and the fidelity of the EBSD measurements. Additional corroboration came in the form of a LDRD study carried out this last year at Lawrence Livermore National Laboratory [12]. In this study, a copper plate was incipiently spalled to obtain a population of large voids in the plate’s interior. Cylindrical samples were then cut from this plate and subsequently compressed in a split-Hopkinson pressure bar at a nominal rate of 3000/s. Some of the voids closed but most of them were still clearly evident. This lends support to the idea that there was no large void fraction opened up during the initial loading of the discs that was subsequently welded shut during deceleration.

V. Conclusions

There are several conclusions to be drawn from the explosively driven disc experiments, their simulations and post-mortem examinations. First, it appears that the damage process in these experiments is more consistent with void sheeting or coalescence along strain localizations than it is with void nucleation and coalescence from high hydrostatic tensile stresses under the classical spall assumption. It is dangerous to constrain a model to only one damage mechanism when several are physically possible from the applied boundary conditions. Second, the strain-to-failure option in TEPLA seems to adequately capture the macroscopic response of the explosively loaded discs. While TEPLA may still be producing too much damage and failing too many elements, it is returning results that are closer to being experimentally consistent.

Third, this study has reinforced previous reports that question the use of the free surface velocity as a stand alone measure of the state of the interior of a dynamically loaded structure. Multiple proposed internal details can all lead to experimentally consistent free surface velocity profiles. VISAR results must be supported with some other independent metrics such as post-mortem examination or proton or x-ray radiography. Fourth, it is an ill-conceived practice to use 'one-dimensional' plate-on-plate experiments to derive failure laws for materials and loading geometries that can fail in a completely different manner.

References

1. Walsh, J.M., Oblique Interactions of Detonation Waves with Explosive/Metal Interfaces, LA-9612-MS, (December 1982).

2. Johnson, J.N. and Addessio, F.L., Tensile plasticity and ductile fracture, Journal of Applied Physics, **64**, pp. 6699-6712, (1988).

3. Johnson, J.N. and Addessio, F.L., Rate-dependent ductile failure model, Journal of Applied Physics, **74**, pp. 1640-1648, (1993).

4. Thissell, W.R., Zurek, A.K., Macdougall, D.A.S. and Tonks, D., Damage evolution and damage model validation in spalled tantalum, Journal de Physique IV, **10**, pp. Pr9-769-774, (2000).

5. Johnson, G.R. and Holmquist, T.J., Test Data and Computational Strength and Fracture Model Constants for 23 Materials Subjected to Large Strains, High Strain Rates, and High Temperatures, LA-11463-MS, (January 1989).

6. Bandstra, J.P. and Koss, D.A., Modeling the ductile fracture process of void coalescence by void-sheet formation, Materials Science and Engineering, **A319-321**, pp. 490-495, (2001).

7. Rogers, H.C., The Effect of Material Variables on Ductility, in <u>Ductility</u>, American Society for Metals, (Metals Park, Ohio), pp. 31-61, (1968).

8. Rogers, H.C., The Tensile fracture of Ductile Metals, Transactions of TMS of AIME, **218**, pp. 498-506, (1960).

9. McClintock, F.A., Kaplan, S.M. and Berg, C.A., Ductile Fracture By Hole Growth in Shear Bands, International Journal of Fracture Mechanics, **2**, pp. 614-627, (1966).

10. McClintock, F.A., A Criterion for Ductile Fracture by the Growth of Holes, ASME Journal of Applied Mechanics, **35**, pp. 363-371, 617, (1968).

11. Meyers, M.A., <u>Dynamic Behavior of Materials</u>, John Wiley and Sons, Inc., (New York, New York), 1994.

12. Becker, R., Modeling and Characterization of Recompressed Damaged Materials, LLNL LDRD Progress Report FY02, Personal communication (2003).